Electrical Power and Energy Systems 117 (2020) 105695

Contents lists available at ScienceDirect

Electrical Power and Energy Systems

journal homepage: www.elsevier.com/locate/ijepes

Automatic partial discharge recognition using the cross wavelet transform in high voltage cable joint measuring systems using two opposite polarity sensors

A. Rodrigo Mor, F.A. Muñoz, J. Wu, L.C. Castro Heredia

Delft University of Technology, Electrical Sustainable Energy Department, Delft, the Netherlands

ARTICLE INFO

Keywords:
partial discharges (PD)
Wavelet transform
Cross wavelet transform
Noise separation
high-frequency current transformer (HFCT)
High voltage cable joint

ABSTRACT

This paper presents a new wavelet analysis approach in partial discharges cable joint measurements in noisy environments. The proposed technique uses the Cross Wavelet Transform (XWT) to separate PD signals from noise and external disturbances in partial discharges measurements in cable joints using two opposite polarity sensors. The partial discharge measurements were performed during impulse and superimposed voltages, leading to a huge amount of noise and pulse shaped external disturbances. The XWT foundations, the experimental setup and the XWT methodology proposed are presented together with the results of the recognition of PD originated in the cable joint. In the experiments, 51,898 signals were acquired, in which 733 were PD signals from the joint and 51,165 corresponded to noise or external disturbances. The XWT performance was studied, finding that 97% of the PD signals were correctly separated by the technique proposed. The results demonstrate the effectivity of the XWT in separating PD signals from noise and external disturbances in this particular measuring system configuration.

1. Introduction

Nowadays, Partial Discharges (PD) detection is an essential tool for the diagnosis of high-voltage equipment because of their accuracy to detect and quantify defects and damages in the dielectric insulation, where the detection implies the measurement, acquisition, storage and processing of the PD phenomenon [1]. In general, the most widespread PD detection system is based on electrical measurements, in which the PD signals are acquired in the form of individual or series of electrical pulses.

In offline PD cable field tests and in laboratory tests, capacitive coupled sensors installed at the cable ends are used [2,3]. In cable systems, statistically most of the partial discharges come from either the cable terminations or the cable joints, being necessary to locate them by time domain reflectometry techniques.

In spite of the PD measurement has been exhaustively researched over the years, the separation of PD pulses from noise is one of the main challenges, especially in online applications. Therefore, noise contamination is one of the significant problems of PD detection [4], because noise, disturbances and interferences can give rise to complex Phase Resolved Partial Discharges (PRPD) patterns or clusters, leading to misleading interpretations [5]. For this reason, several studies [1,4,6–13] have focused on the PD pulses separation and denoising techniques for PD measurements. Among these studies, the wavelet transform has been broadly used because is capable of locating time and frequency components allowing the analysis of aperiodic signals with irregular and transition features, such as the partial discharges [1]. In the wavelet analysis techniques, the Discrete Wavelet Transform (DWT) has been used extensively for denoising PD signals. In general, in the DWT denoising, the wavelet coefficients are calculated for a given signal and then the coefficients are passed through a threshold (soft or hard) and followed by the reconstruction of the signal by taking the inverse wavelet transform of the modified DWT coefficients. However, a major problem that most of these denoising techniques face is the ingress of external interferences having time-frequency characteristics similar to the partial discharge signals (pulse shaped disturbances); for instance, periodic pulse shaped interferences from power electronics or another periodic switching [7], PD and corona discharges from the external power system, electrical pulses from switching operations, lightings, etc. This external noise can cause a false indication of PD activity, jeopardising the PD measurements as a diagnostic tool.

To reduce the false indications, in PD measurement systems more than one electrical sensor (HFCTs, UHF antennas, coupling capacitors, etc.) is used, meaning that multiple waveforms are simultaneously acquired, because recording each signal through different sensors may provide extra useful information about the real nature of the waveform recorded. Tools like the correlation and trend analysis can provide the significance of relationships between the signals recorded [14]. Nevertheless, these tools may not detect correlations if the signals are phase shifted; for instance, a phase shift of 180° between the signals

https://doi.org/10.1016/j.ijepes.2019.105695
Received 6 August 2019; Received in revised form 12 September 2019; Accepted 5 November 2019

may appear uncorrelated. The cross-correlation and the cross-spectral analysis can detect the phase shift, but only as average values and in stationary signals. For analysing aperiodic signals with irregular and transition features, the most suitable tool is the Cross Wavelet Transform (XWT) because it exposes regions with high common power and reveals the local relative phase between both signals [14].

The Cross Wavelet Transform is an extension of the wavelet analysis [4], and it is a measure of similarity between two waveforms [15]. It exposes regions with high common power and reveals information about the phase relationship. Therefore, the XWT finds links between two signals, because it gives a measure of the correlation between two time series in the time-frequency domain [4]. Therefore, it may be possible to apply the XWT in the separation of PD signals from noise and external disturbances when multiple sensors are deployed.

The XWT has been used in PD measurements [4,16–18]. In [4] reported the application of cross wavelet analysis in PD measurements, by analysing the common power spectrum between two PD sensors located in the test object. They used the XWT for defect classification using feature extraction and artificial neural networks. The results showed that the defect could be successfully classified by the technique proposed. In [17,18] applied the XWT in PD measurements performed in transformers. They used the cross wavelet to identify regions having high common power between the PD signals measured at different locations in the transformer. Finally, in [16] the XWT was used for the discrimination and localisation of PD using acoustic measurements.

Nevertheless, in these previous studies, the application of XWT techniques for removal of external interferences having time-frequency characteristics similar to the PD pulses has not been examined so far. For this reason, in this paper, the XWT was used to separate PD signals from noise and pulse shaped external disturbances in PD measurements. The PD pulses were originated in a high voltage cable joint during impulse and superimposed voltages. An unconventional partial discharge measuring system, based on two opposite polarity HFCTs installed at the cable joint, was used to localise and measure the PD activity in the joint under the impulse condition. The paper describes the experiment performed, the XWT theory, the methodology proposed and the results of applying it to the data collection.

2. Experimental setup

The PD pulses were measured in a high voltage (HV) cable system, during impulse and superimposed voltages. An unconventional partial discharge measuring system was deployed to localise and measure the PD activity in the HV cable joint under the impulse condition. In the cable joint, an artificial defect has been introduced to produce partial discharges. The artificial defect was created by manipulating the joint, in which the connector in the joint was prepared in such a way that the cable can be pulled out of the joint. To create the PD source, the cable was pulled 10 mm out of the joint at one joint side. The set up was tested under AC, showing a sufficient PD level for research purposes.

The experiments were conducted on the test circuit shown in Fig. 1, which consisted of the test object, the voltage supplies and the PD measuring system detailed in Fig. 2. The test object was a 150 kV cross-linked polyethylene (XLPE) extruded cable with two dry type outdoor terminations named termination 1 and 2, and a pre-moulded joint in between. A 380 V/150 kV test transformer supplied the AC voltage. The impulses were applied using a Marx generator connected to the HV cable system. Fig. 1 shows a simplified sketch of the test setup. Detailed information on the setup, the artificial defect, and the PD measuring system installed at the joint can be found at [19].

Two identical HFCTs (gain of 3 mV/mA and a bandwidth of 100 kHz–40 MHz) were installed at the cable joint position to measure the PD activity. The PD signals acquired by the two HFCTs were first filtered and then transmitted through two 20-m identical coaxial cables to a digital oscilloscope Tektronix MSO58. The filters in combination with transient voltage suppressors were connected between the sensors

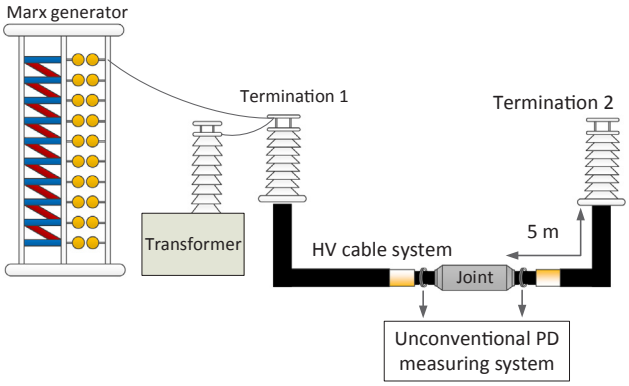

Fig. 1. Simplified test setup and test object.

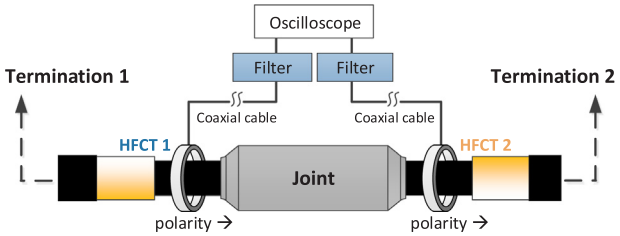

Fig. 2. Two HFCTs installed at two ends of cable joint.

and the oscilloscope to prevent oscilloscope damage due to the induced voltages during the high voltage transients. The oscilloscope was set at 1.25 GS/s with 250 MHz bandwidth. The acquisition of the signals coming from the sensors was made using the Fast Frame Acquisition Mode because it allows capturing multiple signals at the sampling rate mentioned before. Each signal was recorded individually in a frame with a record length of 2.02 µs.

The HFCTs were installed at both ends of the joint with the same polarity, as shown in Fig. 2. In this arrangement, when a PD occurs externally to the cable joint (i.e. near termination 1 or termination 2), the PD signals measured by both HFCT have the same polarity and similar magnitudes; this would also be the case for external disturbances coming from outside the cable joint. In a different scenario, if a PD occurs in the cable joint, the PD pulse is generated between the two HFCTs, and it propagates in both directions, which causes that the PD pulses measured by the HFCTs have opposite polarities and similar magnitudes. By using this measuring system, a signal measured by both HFCTs is considered a PD signal when it met these two criteria: the peak occurs around the same time in both HFCTs, and the HFCTs signals have different polarities.

The test was performed under laboratory conditions, causing few electromagnetic disturbances and low background noise before the impulse. However, the impulse voltage in the Marx generator produces itself an electromagnetic interference that causes a huge amount of noise and disturbances. Therefore, the challenge is to detect and identify individual partial discharges during the impulse moment.

This work uses a collection of 10 measurement results, as is shown in Table 1; 51,898 signals were acquired by the oscilloscope (using the Fast frame acquisition mode), and only 733 signals (1.41%) corresponded to PD pulses. All the signals were checked manually to identify PD signals that met the two criteria mentioned before. Fig. 3 shows a characteristic PD pulse measured by both HFCTs, and Fig. 4 presents a pulse shaped external disturbance acquired by the measuring system; Fig. 5 presents a zoom-in of Fig. 4. In the PD pulse, it is possible to notice that the peaks appear around the same time (around 433 ns), and the signals have different polarities in the first tens of nanoseconds. After that, the opposite polarity in the signals is lost due to signal overlapping of the multiple reflections in the cable. On the other hand,

Table 1
Data collection overview.

Test	Signals acquired	PD pulses	Noise + external disturbances
1	11,261	47	11,214
2	1212	85	1127
3	2188	75	2113
4	2475	50	2425
5	5256	109	5147
6	15,759	184	15,575
7	2047	33	2014
8	6969	23	6946
9	2011	51	1960
10	2720	76	2644
Total	51,898	733 (1.41%)	51,165 (94.6%)

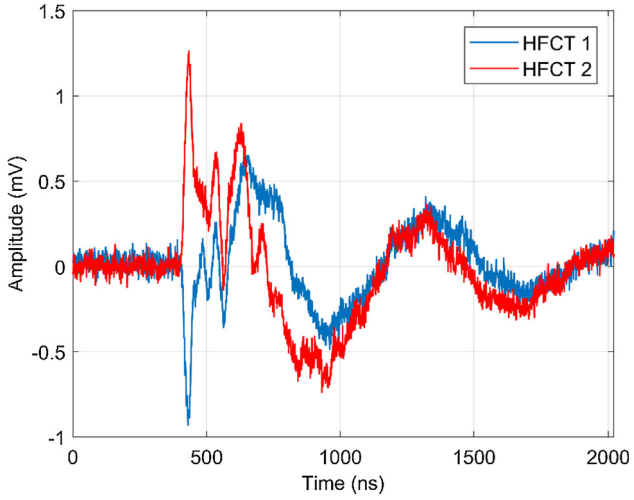

Fig. 3. PD pulse from the joint.

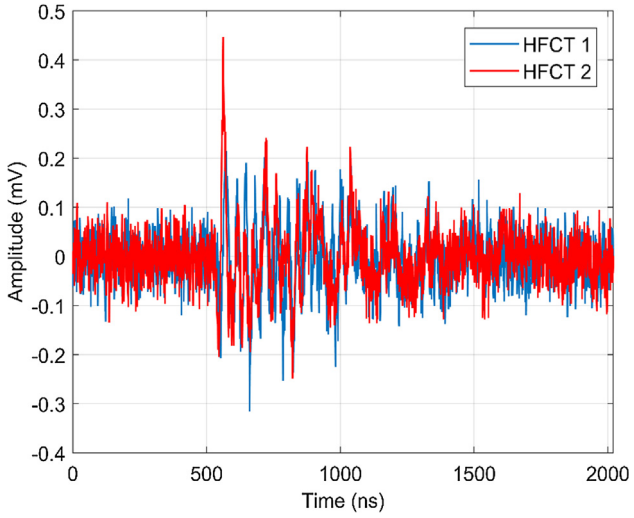

Fig. 4. Pulse shaped external disturbance.

the external disturbance does not meet the criteria because the signals have the same polarity.

3. Cross wavelet transform

The Continuous Wavelet Transform (CWT) is a mathematical tool that transforms a time domain signal to a time-scale domain [20]. The wavelet is a function with zero mean, which is localized in both frequency and time [21]. The CWT of time series (y_n, $n = 1, \ldots, N$) with uniform time steps δt, is defined as the convolution of y_n with the normalized and scaled wavelet [21]. The CWT of y_n is defined as:

$$W_n^Y[s, n] = \sqrt{\frac{\delta t}{s}} \sum_{n=1}^{N} y_{n'} \psi_0[(n' - n)\frac{\delta t}{s}] \quad (1)$$

where ψ_0 is the wavelet, and s is the scale.

The CWT is a powerful tool for analysing localised non-periodic oscillations in a time series, or for feature extraction purposes. However, the Cross Wavelet Transform (XWT) is more appropriate for finding an existing link between two-time series, because it gives a measure of the correlation between two time series in the time-frequency domain [4]. The XWT of two-time series x_n and y_n is defined as:

$$W^{YX}[s, n] = W^Y[s, n] W^{X*}[s, n] \quad (2)$$

where $W^Y[s, n]$ and $W^X[s, n]$ are the CWT of y_n and x_n, respectively, and the operator * means complex conjugate. The $W^{YX}[s, n]$ argument can be interpreted as the local relative phase between both time series [21]. The $W^{YX}[s, n]$ absolute value is commonly displayed by means of the scalogram, which represents the percentage of energy for each scale. The scalogram is defined in Eq. (3).

$$SC^{YX}[s, n] = 100 * \frac{|W^{YX}[s, n]|}{\sum_{s=1}^{M} \sum_{n=1}^{N} |W^{YX}[s, n]|} \quad (3)$$

where M is the total number of scales.

Taking into account that the PD measuring system has two HFCTs, the XWT may help us to automatically check the correlation between the signals acquired. For instance, in a PD signal, having the peaks around the same time, we would expect that the XWT shows that both PD pulses have high common power around the time where the PD peaks occur. Additionally, for a PD originated in the joint like the one in Fig. 3, the XWT argument would display a local relative phase between both PD signals near to 180°, because the PD signal has different polarities in the two HFCTs.

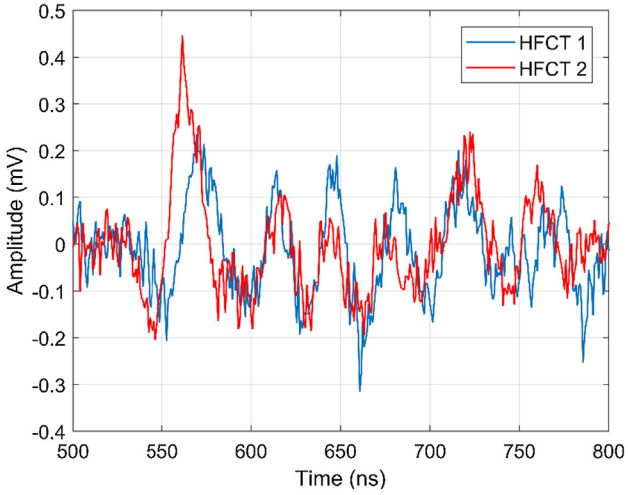

Fig. 5. Zoom-in pulse shaped external disturbance.

4. Wavelet and scales selection

The XWT is a useful tool to identify the regions with a high correlation between two signals, but its outcome relies on the wavelet and the number of scales chosen. In a similar study in PD identification [4], the Morlet wavelet was found as the most suitable option for feature extraction from noisy signals. Nevertheless, this selection depends on the nature of the problem. For that reason, in this study, different complex wavelets and scales were tested, finding the best performance with 16 scales and the complex gaussian 4 (cgau4) wavelet. Only complex wavelets were tested because they return information about

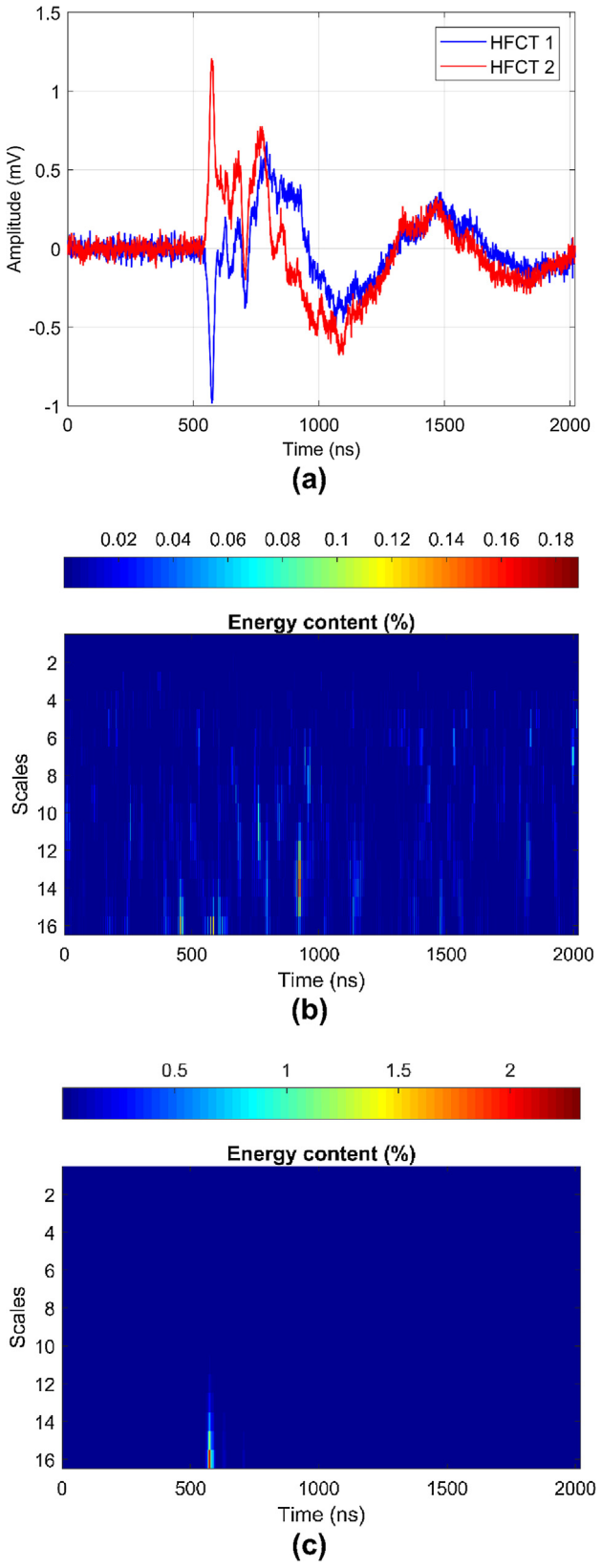

Fig. 6. (a) PD signals, (b) Morlet scalogram, (c) cgau4 scalogram.

both amplitude and phase, which is needed to get the local relative phase between the signals in both HFCTs.

Different wavelets and scales were tested following the next steps:

- From the collection of data shown in Table 1, 10 PD pulses were randomly chosen from both HFCTs. In an alternative way, it is possible to use PD calibration pulses injected in the cable joint.
- For each PD signal, the XWTs and the scalograms were obtained using different wavelets and scales. In total, 7 complex wavelets (cgau1, cgaus2, cgau3, cgau4, Morlet, complex Morlet 1-1 and complex Morlet 1-2) and 3 different scales (8, 16, and 32) were analysed. For instance, Fig. 6 shows a PD signal measured by both PD sensors and its respective scalogram for the wavelets Morlet and cgau4. The scalogram colorbar indicates the percentage of energy.
- The performance of each wavelet mother and scales was analysed based on the percentage of energy around the first peak of the PD signal. It is desired to have a high energy concentration around the first peak and relatively low energy in the remaining part of the signal. In Fig. 6c, the scalogram for cgaus4 shows that the energy is higher around the first peak than in the remaining signal, whereas the scalogram for Morlet presents a more widespread energy distribution, Fig. 6b. Among the wavelets and the different scales examined, the cgau4 in combination with 16 scales has shown the best performance.

5. Methodology

The aim of the present work is developing a tool capable of separating PD pulses from a collection of data which contains multiple types of disturbances and noise for this particular application. The methodology followed is presented below.

5.1. Butterworth filter

First, the signals were filtered out using a Butterworth band-pass filter order 2, with bandwidth 0.1–40 MHz, to eliminate the high-frequency noise measured by the acquisition system. This frequency bandwidth corresponds to the HFCT bandwidth.

5.2. XWT and scalograms

After filtering the signals, the XWTs and the scalograms were calculated for each of the 51,898 signals. The scalogram for the PD pulse in Fig. 3 is shown in Fig. 7, where the percentage of energy for all the 16 scales is presented. Fig. 8 depicts the scalogram for the external disturbance in Fig. 4.

It is possible to notice that in both signals, there is a high concentration of the energy around the first peak of the signals. As expected, both scalograms show an strong existing link between the

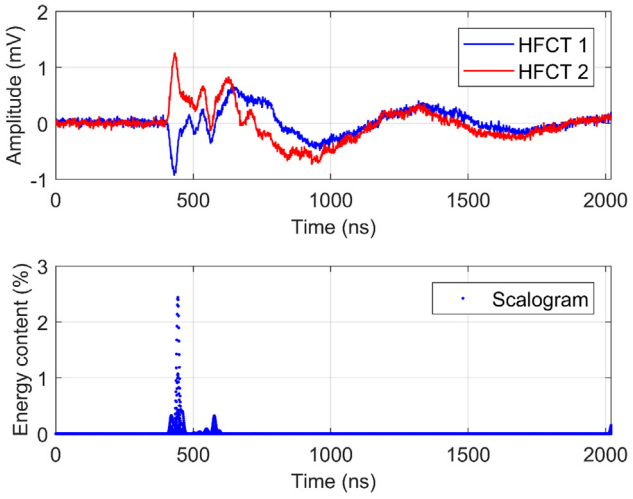

Fig. 7. Scalogram PD signal.

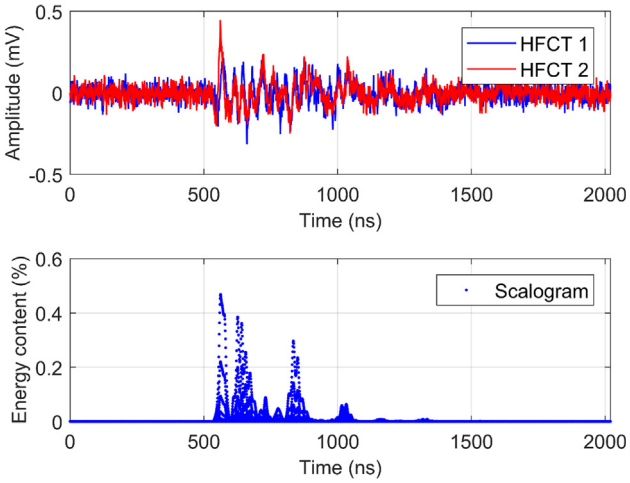

Fig. 8. Scalogram pulse shaped external disturbance.

signals measured by both HFCTs. However, these scalograms do not provide information about the relative phase of the signals measured, which is relevant for the PD identification (opposite polarities).

5.3. Local relative phase

The XWT argument was calculated to obtain the local relative phase. As it was mentioned, this parameter measures the relative phase between both HFCT signals and, therefore, it varies from 0° to 180°.

Considering that a PD pulse measured by both PD sensors has opposite polarity, it is expected a local relative phase near to 180° around the first peak. However, a 180° local phase is an idealisation that helps to explain the nature of the problem, but because of the small delays in both HFCT signals, manufacturing differences and the discretisation, a lower local phase would be expected. Therefore, the scalogram indexes corresponding to a local relative phase higher than 145° were selected and stored in a new variable named SC145. The scalogram SC145 corresponding to the PD signal is presented in Fig. 9, whereas Fig. 10 shows the SC145 corresponding to the external disturbance.

In Fig. 9, the energy having a local phase higher than 145° is still highly concentrated around the PD pulse first peak, indicating that both HFCTs signals have different polarities; Fig. 11 shows the PD pulses indexes having the XWT argument higher than 145°. On the other hand, the energy content in the external disturbance does not have a local relative phase higher than 145°, pointing out that both signals have the

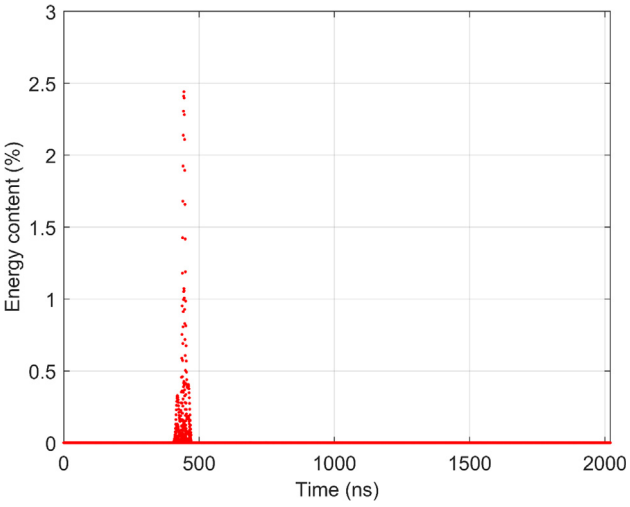

Fig. 9. Scalogram SC145 of the PD signal.

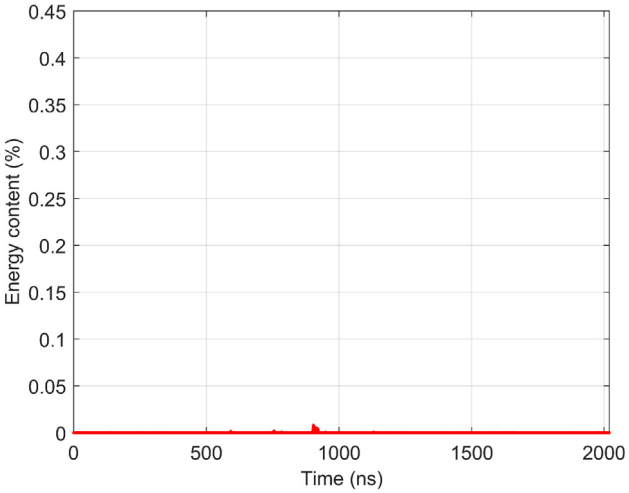

Fig. 10. External disturbance scalogram SC145.

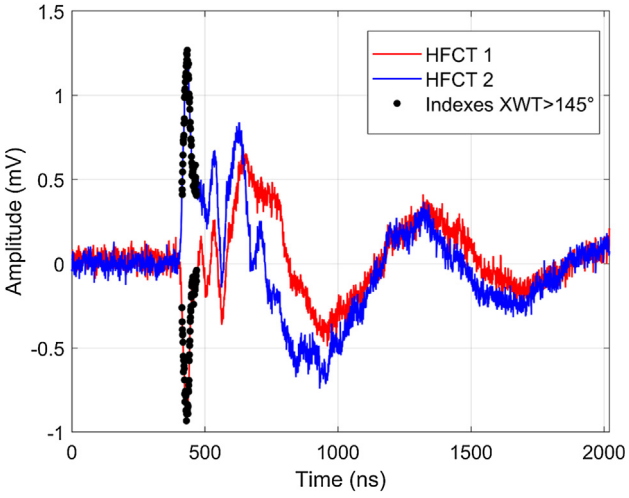

Fig. 11. PD signal indexes having a XWT argument higher than 145°.

same polarity.

5.4. PD automatic extraction

A signal is classified and separated as a PD signal if the energy percentage SC145, in some of the 16 scales, is higher than an established threshold. In this study, the threshold was arbitrarily adjusted at 0.5% after checking the PD pulses scalograms. In Fig. 12 is presented the applied method scheme.

6. Results

An algorithm was developed based on the methodology presented in chapter 5 and was applied to the data collection. Table 2 shows the results.

Overall, 97% of the PD signals were correctly identified, which

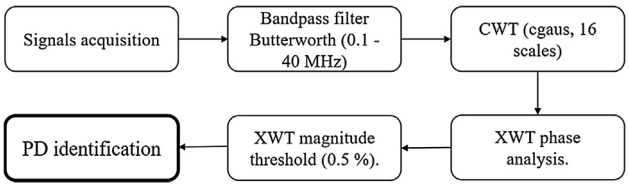

Fig. 12. Scheme to PD identification.

Table 2
Results data analysis.

Test	PD pulses detected	PDs not detected	External disturbance captured (PD false detection)
1	51	0	4
2	85	0	0
3	76	1	2
4	50	0	0
5	111	0	2
6	191	1	8
7	36	0	3
8	24	1	2
9	51	0	0
10	77	0	1
Total	752	3 (0.4%)	22 (2.93%)

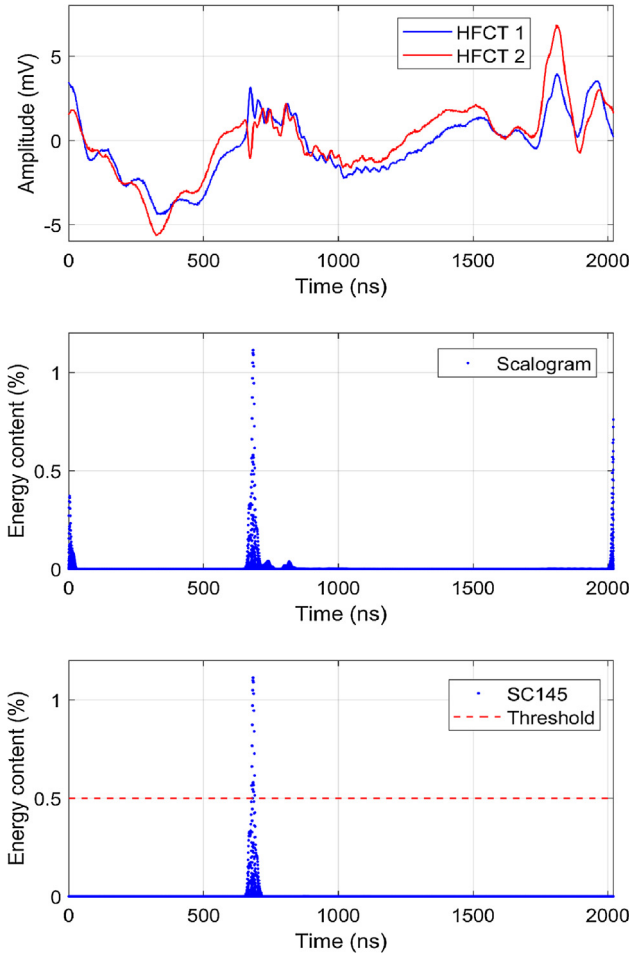

Fig. 13. XWT analysis of a PD signal immersed in noise.

means that 2.93% of the signals detected corresponded to noise or external disturbances. Additionally, only 3 PD signals (0.4%) were not extracted by the algorithm.

Among the PD collected by the algorithm, the signal in Fig. 13 represents an excellent example to demonstrate the capabilities of the cross wavelet transform for PD detection. The PD pulse appears around the 700 ns, and in both HFCTs, it has a lower magnitude than the surrounding noise, meaning that the PD pulse has a low signal to noise ratio (SNR). In this signal, the scalogram shows a high correlation around the PD pulse, but also at the beginning and final part of the signal. However, the SC145 presents the energy content mainly concentrated around the PD peaks, reaching energy percentages three times higher than the threshold.

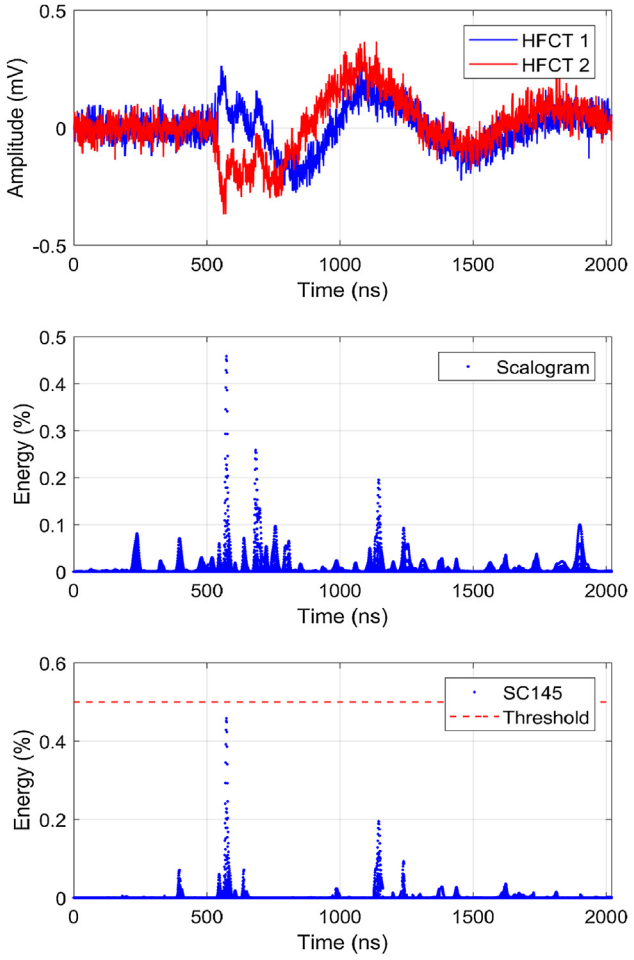

Fig. 14. PD signal not detected by the algorithm.

Nevertheless, some PD signals with a low SNR may be not detected by the algorithm, which is the case depicted in Fig. 14. The correlation energy is more spread in the whole signal, and not mainly concentrated around the PD pulse, causing SC145 values lower than the threshold.

Regarding the noise wrongly captured by the algorithm, a characteristic example is shown in Fig. 15. The external disturbance shows a high correlation at the beginning of the signal with a local relative phase higher than 145°. This type of disturbance, having a high SC145 at the signals ends, has been a recurrent source of false positives. The reason is the signal segmentation which, in some cases, creates this singularity at the signal ends.

7. Conclusions

A XWT based analysis has been proven to be an effective tool in this particular application to identify PD pulses from the cable joint. The results showed that the use of this technique succeeds in the separation of PD signals from noise and pulse shaped external disturbances. Among the data collected (51898 signals), 97% of the PD signals were correctly identified, 2.93% of the signals detected were false positives, and 0.4% of the PD signals were not separated. The false positives detected were caused by the combination of the signal segmentation and noise. The wavelet complex Gaussian 4, cgau4, in 16 scales, has shown the best performance in the identification of PD signals in this particular application. It was found that both the PD signals and the external disturbances have a high energy concentration around the signal peaks. The XWT relative phase can be used to discriminate PD signals with opposite polarity, like the ones expected from the joint due to the HFCTs arrangement. The calculation of the signal indexes

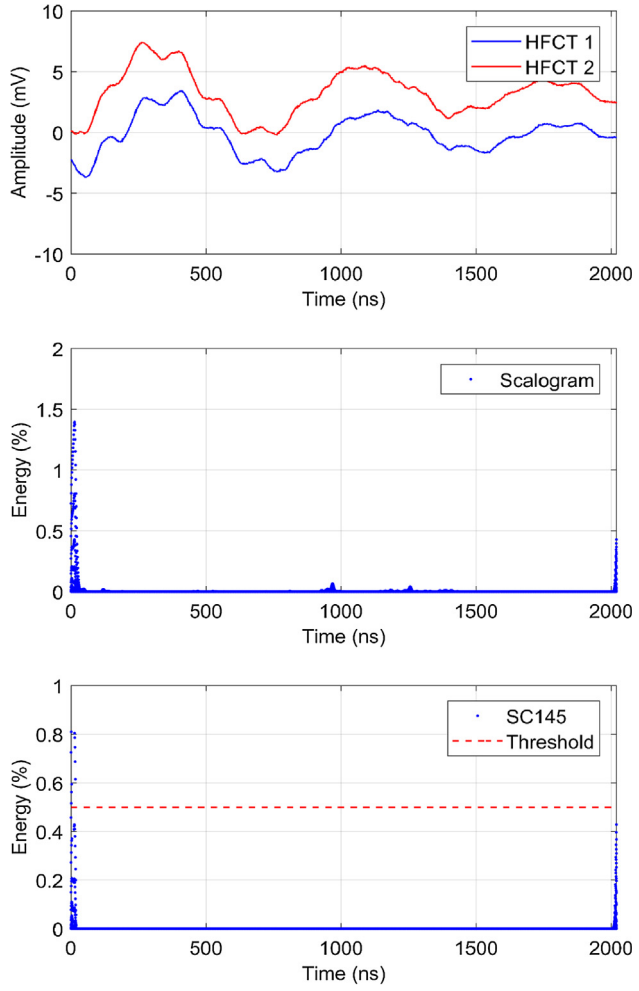

Fig. 15. False positive detected by the algorithm.

corresponding to relative phases bigger than 145° identifies the portion of the signals corresponding to real PD pulses from the joint.

Declaration of Competing Interest

The authors declare that they have no known competing financial interests or personal relationships that could have appeared to influence the work reported in this paper.

Acknowledgment

Authors would like to thank TenneT B.V. of the Netherlands for partially funding this project.

References

[1] Ma X, Zhou C, Kemp IJ. Interpretation of wavelet analysis and its application in partial discharge detection. IEEE Trans Dielectr Electr Insul 2002;9(3):446–57.
[2] Mor AR, Morshuis PHF, Llovera P, Fuster V, Quijano A. Localization techniques of partial discharges at cable ends in off-line single-sided partial discharge cable measurements. IEEE Trans Dielectr Electr Insul 2016;23(1):428–34.
[3] Rodrigo A, Llovera P, Fuster V, Quijano A. High performance broadband capacitive coupler for partial discharge cable tests. IEEE Trans Dielectr Electr Insul 2013;20(2):479–87.
[4] Dey D, Chatterjee B, Chakravorti S, Munshi S. Cross-wavelet transform as a new paradigm for feature extraction from noisy partial discharge pulses. IEEE Trans Dielectr Electr Insul 2010;17(1):157–66.
[5] Rodrigo Mor A, Castro Heredia LC, Muñoz FA. Effect of acquisition parameters on equivalent time and equivalent bandwidth algorithms for partial discharge clustering. Int J Electr Power Energy Syst 2017;88:141–9.
[6] Zhang H, Blackburn TR, Phung Bt, Sen D. A novel wavelet transform technique for on-line partial discharge measurements. 1. WT de-noising algorithm. IEEE Trans Dielectr Electr Insul 2007;14(1):3–14.
[7] Satish L, Nazneen B. Wavelet-based denoising of partial discharge signals buried in excessive noise and interference. IEEE Trans Dielectr Electr Insul 2003;10(2):354–67.
[8] Zhu M-X, et al. Partial discharge signals separation using cumulative energy function and mathematical morphology gradient. IEEE Trans Dielectr Electr Insul 2016;23(1):482–93.
[9] Alvarez F, Ortego J, Garnacho F, Sanchez-Uran MA. A clustering technique for partial discharge and noise sources identification in power cables by means of waveform parameters. IEEE Trans Dielectr Electr Insul 2016;23(1):469–81.
[10] Albarracin R, Robles G, Martinez-Tarifa JM, Ardila-Rey J. Separation of sources in radiofrequency measurements of partial discharges using time–power ratio maps. ISA Trans 2015;58:389–97.
[11] Robles G, Parrado-Hernández E, Ardila-Rey J, Martínez-Tarifa JM. Multiple partial discharge source discrimination with multiclass support vector machines. Expert Syst Appl 2016;55:417–28.
[12] Ardila-Rey JA, Martinez-Tarifa JM, Robles G. Automatic selection of frequency bands for the power ratios separation technique in partial discharge measurements: part II, PD source recognition and applications. IEEE Trans Dielectr Electr Insul 2015;22(4):2293–301.
[13] Shim I, Soraghan JJ, Siew WH. Detection of PD utilizing digital signal processing methods. Part 3: Open-loop noise reduction. IEEE Electr Insul Mag 2001;17(1):6–13.
[14] Prokoph A, El Bilali H. Cross-wavelet analysis: a tool for detection of relationships between paleoclimate proxy records. Prog. Geomathematics 2008;499–511.
[15] Banerjee S, Member S, Mitra M. Application of cross wavelet transform for ECG pattern analysis and classification. IEEE Trans Instrum Meas 2014;63(2):326–33.
[16] Biswas S, Dey D, Chatterjee B, Chakravorti S. Cross-spectrum analysis based methodology for discrimination and localization of partial discharge sources using acoustic sensors. IEEE Trans Dielectr Electr Insul 2016;23(6):3556–65.
[17] Suryavanshi H, Velandy J, Sakthivel M. Wavelet power ratio signature spectrum analysis for prediction of winding insulation defects in transformer and shunt reactor. IEEE Trans Dielectr Electr Insul 2017;24(4):2649–59.
[18] Dey D, Chatterjee B, Chakravorti S, Munshi S. Rough-granular approach for impulse fault classification of transformers using cross-wavelet transform. IEEE Trans Dielectr Electr Insul 2008;15(5):1297–304.
[19] Wu J, Rodrigo Mor A, van Nes PVM, Smit JJ. Measuring method for partial discharges in a high voltage cable system subjected to impulse and superimposed voltage under laboratory conditions. Int J Electr Power Energy Syst 2020;115:105489.
[20] Maraun D, Kurths J, Holschneider M. Nonstationary Gaussian processes in wavelet domain: synthesis, estimation, and significance testing. Phys Rev E 2007;75(1):016707.
[21] Grinsted A, Moore JC, Jevrejeva S. Application of the cross wavelet transform and wavelet coherence to geophysical time series. Nonlinear Process Geophys 2004;11(5/6):561–6.

Armando Rodrigo Mor is an Industrial Engineer from Universitat Politècnica de València, in Valencia, Spain, with a Ph.D. degree from this university in electrical engineering. During many years he has been working at the High Voltage Laboratory and Plasma Arc Laboratory of the Instituto de Tecnología Eléctrica in Valencia, Spain. Since 2013 he is an Assistant Professor in the Electrical Sustainable Energy Department at Delft University of Technology, in Delft, The Netherlands. His research interests include monitoring and diagnostic, sensors for high voltage applications, high voltage engineering, and HVDC.

Fabio Andrés Muñoz was born in Cali, Colombia, in 1988. He received the B.S. degree in electrical engineering from the Universidad del Valle, Cali, in 2011, and a PhD degree in 2017 from the same university. Currently, he is a postdoc in the Electrical Sustainable Energy Department at Delft University of Technology, in Delft, The Netherlands. His main research interests are focused on high voltage engineering, insulation diagnostics and applied electromagnetism.

Jiayang Wu was born in Nanjing, China in 1988. She received the BSc degree in electrical engineering from the Southeast University, Nanjing, China, in 2010, and the MSc degree in electrical power engineering from the RWTH Aachen University of Technology, Aachen, Germany in 2013. She is currently a Ph.D candidate in the Electrical Sustainable Energy Department at Delft University of Technology, Delft, The Netherlands. Her current research focuses on the effects of transients on the high voltage cable systems.

Luis Carlos Castro was born in Cali, Colombia in 1986. He received the Bachelor and PhD degree in electrical engineering from Universidad del Valle, Cali, in 2009 and 2015 respectively. Currently, he is a post-doc in the Electrical Sustainable Energy Department at Delft University of Technology, in Delft, The Netherlands. His research interests include high-voltage technology, partial discharge testing, accelerated aging of stator insulation and monitoring and diagnostic tests.